Influence of specularly reflecting boundaries on radiation trapping in a plane-parallel slab

Andreas F. Molisch, Bernhard P. Oehry, Walter Schupita, Brigitte Sumetsberger, and Gottfried Magerl
Institut für Nachrichtentechnik und Hochfrequenztechnik, Technische Universität Wien, Gußhausstraße 25/389, A-1040 Vienna, Austria
(Received 16 February 1994)

We consider radiation trapping in a plane-parallel slab with specularly reflecting boundaries. The reflection coefficient of the walls can be different at the two sides of the slab, and may depend on the angle and frequency of the radiation. We derive a closed-form Green's function, and give an efficient method for its evaluation. We show that, in most cases, higher-order modes have practically no influence on the temporal behavior of the emergent radiation when the reflection coefficients at both walls are high, but that they are important when only one wall is highly reflecting. We also investigate the difference between diffuse and specular reflection. For center-of-line opacities k_0L exceeding 0.5, the difference in the lowest-order trapping factor is quite small (less than 3% for Doppler line shapes and less than 6% for Lorentzian shapes). Trapping calculations can therefore be simplified by using the formulas for specular instead of diffuse reflection.

PACS number(s): 32.50.+d

I. INTRODUCTION

Resonance radiation is emitted by excited atoms when they radiatively decay to the ground state. In an atomic vapor cell, these atoms are surrounded by atoms of the same kind, so that the radiation can be absorbed and reemitted many times before it reaches the boundaries of the vapor cell. This effect is known as "imprisonment of resonance radiation" or "radiation trapping" [1]. It leads to an increase in the apparent lifetime of the excited atoms and distorts the spectral line shape of the emergent radiation. Analysis of radiation trapping is thus of importance in chemical physics, spectroscopy [2], and atomic line filters [3]. Mathematically, radiation trapping is described by the Holstein equation [4], a rate equation for the density of the excited-state atoms.

In the study of radiation trapping, the most important geometry is the plane-parallel slab (also known as the infinite slab), extending infinitely in the x and y directions and from $-L/2$ to $L/2$ in the z direction. The slab often is a good approximation for actual vapor cells [5] and the geometry treated most frequently in the literature. During the past 30 years, there have been a number of papers that considered trapping in a slab with partially reflecting walls. The first such work was done by Weinstein [6], who considered diffusely reflecting walls with the same reflection coefficients at both walls. In 1964, Tkachuk [7] gave the Holstein equation for a slab with *specularly* reflecting walls, also with the same reflection coefficient at both walls. However, this important contribution remained largely unnoticed; later papers again assumed diffusely reflecting walls, although they are of less practical importance. In Ref. [8,9], Weinstein's results were evaluated numerically.

Recently, Colbert and Wexler [10] generalized Weinstein's results and derived an equation for the case that the (diffuse) reflection coefficients of the slab walls are different (nonuniform). Their work stimulated us to complete the picture by generalizing Tkachuk's results on specularly reflecting walls to nonuniform wall reflectivities, i.e., we give the Holstein equation for specularly reflecting walls where the reflection coefficients at the two walls are different, and can depend on angle and frequency. We furthermore give a method for the efficient evaluation of this Holstein equation and compare the results for diffusely and specularly reflecting walls.

II. THEORY

For the derivation of the Holstein equation, we make the following simplifying assumptions: (i) the flight time of the photons is much shorter than the natural lifetime τ of the excited-state atoms, (ii) complete frequency redistribution is valid, (iii) the distribution of ground-state atoms is homogeneous, (iv) no saturation effects occur, (v) particle diffusion is negligible, and (vi) we have a two-level atom. These assumptions are discussed in Refs. [5] and [10] and are often fulfilled in laboratory situations.[1]

With these assumptions, the Holstein equation reads

$$\frac{\partial n(z,t)}{\partial t} = -\frac{1}{\tau} n(z,t) + \frac{1}{\tau} \int_{-L/2}^{L/2} n(z',t) G(z,z') dz' , \qquad (1)$$

where n is the excited-state density, τ is the natural lifetime of the excited-state atoms, and the Green's function $G(z,z')$ is the probability that a photon emitted at z' is reabsorbed at z. Solutions of Eq. (1) are of the form

$$n(z,t) = \sum_j \alpha_j \Psi_j(z) \exp\left[-\frac{t}{g_j \tau} \right] , \qquad (2)$$

where the ψ_j are the eigenmodes, g_j the associated trap-

[1]We will see below that the effective size of a cell with reflecting walls (reflection coefficient R) is $L/(1-R)$. The condition for the validity of (i) is thus $L/(1-R) \ll \tau c$.

ping factors, and α_j the expansion coefficients of the initial distribution into the eigenmodes. Equation (2) expresses the fact that an initial distribution of excited atoms $n(z,0)$ can be expanded into eigenmodes that independently decay with individual exponential time constants that are each eigenmode's trapping factor times the natural lifetime of the excited state.

In the case of completely transparent boundaries of the vapor cell, $G(z,z')$ is [11]

$$G^{\text{no refl}}(|z-z'|) = C_x \frac{k_0}{2} \int_1^\infty \int_{-\infty}^\infty \frac{k^2(x)}{u} \exp[-k_0|z-z'|k(x)u] \times dx\, du \ , \quad (3)$$

where k_0 is the line-center absorption coefficient, $k(x)$ is the line shape, x is the normalized frequency, and $C_x = 1/\int k(x)dx$. The angle integration is performed over u, where $u = 1/|\cos\vartheta|$ and ϑ is the angle between the z axis and the photon flight direction. The problem now lies in finding the Green's function for reflecting boundaries.

We assume quite general boundary conditions: the reflection coefficients R_+ and R_- (at $L/2$ and $-L/2$, respectively) can depend on angle and frequency, $R_+ = R_+(x,u)$ and $R_- = R_-(x,u)$. We note that u is not changed by a specular reflection. Photons that are emitted at z' toward the right wall (i.e., the wall at $z = L/2$), are reflected once, and are then reabsorbed at z have to cover the distance

$$u(L/2-z') + u(L/2-z) \ .$$

The Green's function for these photons is

$$G^{\text{one refl}}(z,z') = C_x \frac{k_0}{2} \int_1^\infty \int_{-\infty}^\infty R_+(x,u) \frac{k^2(x)}{u} \times \exp[-k_0(L-z-z')k(x)u]dx\, du \ . \quad (4)$$

Similar terms can be written for photons that are reflected once at the left wall, for photons that are reflected once at $L/2$ and once at $-L/2$, twice at $L/2$ and once at $-L/2$, and so on. These Green's functions are then all added up. If arranged appropriately, we get four infinite series that can be summed up analytically. We thus get

$$\begin{aligned} G^{\text{refl}}(z,z') = {} & G^{\text{no refl}}(|z-z'|) \\ & + C_x \frac{k_0}{2} \int_1^\infty \int_{-\infty}^\infty \frac{k^2(x)}{u} \frac{R_+(x,u)R_-(x,u)}{1-R_+(x,u)R_-(x,u)e^{-2k_0Lk(x)u}} e^{-k_0k(x)(2L+z-z')u} dx\, du \\ & + C_x \frac{k_0}{2} \int_1^\infty \int_{-\infty}^\infty \frac{k^2(x)}{u} \frac{R_+(x,u)R_-(x,u)}{1-R_+(x,u)R_-(x,u)e^{-2k_0Lk(x)u}} e^{-k_0k(x)(2L+z'-z)u} dx\, du \\ & + C_x \frac{k_0}{2} \int_1^\infty \int_{-\infty}^\infty \frac{k^2(x)}{u} \frac{R_+(x,u)e^{-k_0k(x)(L-z-z')u}}{1-R_+(x,u)R_-(x,u)e^{-2k_0Lk(x)u}} dx\, du \\ & + C_x \frac{k_0}{2} \int_1^\infty \int_{-\infty}^\infty \frac{k^2(x)}{u} \frac{R_-(x,u)e^{-k_0k(x)(L+z+z')u}}{1-R_+(x,u)R_-(x,u)e^{-2k_0Lk(x)u}} dx\, du \ . \end{aligned} \quad (5)$$

Equation (5) gives, for the first time, the Green's function in a slab with specularly reflecting walls with different reflectivities of the two walls. The reflection coefficients may depend on angle and frequency.

For the numerical evaluation of Eq. (1), we divide the slab into S substripes and assume that n is constant within each substripe. Mathematically, this means approximating n by a set of S orthogonal rectangular pulse functions with unknown amplitudes. Equation (1) then reduces to a system of homogeneous algebraic equations,

$$n_k(1-1/g) - \sum_{m=0}^{S-1} n_m A_{km} = 0 \quad \text{with} \quad A_{km} = \int_{z_m-\Delta/2}^{z_m+\Delta/2} G^{\text{refl}}(z_k,z')dz' \ , \quad (6)$$

when the z_m are the center coordinates of the substripes and Δ is the constant width. We found a particularly advantageous formulation for the matrix elements A_{km}:

$$
\begin{aligned}
I_i^a &= C_x \int_{-\infty}^{\infty} k(x)\{1-\mathrm{Ei}_2[k_0 k(x)\Delta/2]\}dx \quad \text{for } i=0 \\
&= \frac{C_x}{2}\int_{-\infty}^{\infty} k(x)\{\mathrm{Ei}_2[(i-0.5)k_0 k(x)\Delta]-\mathrm{Ei}_2[(i+0.5)k_0 k(x)\Delta]\}dx \quad \text{for } i\neq 0 , \\
I_i^b &= \frac{C_x}{2}\int_1^{\infty}\int_{-\infty}^{\infty}\frac{k(x)}{u^2}\frac{R_+(x,u)R_-(x,u)e^{-k_0 Lk(x)u}}{1-R_+(x,u)R_-(x,u)e^{-2k_0 Lk(x)u}}[e^{-k_0 k(x)(i-0.5)\Delta u}-e^{-k_0 k(x)(i+0.5)\Delta u}]dx\,du , \\
I_i^c &= \frac{C_x}{2}\int_1^{\infty}\int_{-\infty}^{\infty}\frac{k(x)}{u^2}\frac{R_+(x,u)}{1-R_+(x,u)R_-(x,u)e^{-2k_0 Lk(x)u}}[e^{-k_0 k(x)(i-0.5)\Delta u}-e^{-k_0 k(x)(i+0.5)\Delta u}]dx\,du , \\
I_i^d &= \frac{C_x}{2}\int_1^{\infty}\int_{-\infty}^{\infty}\frac{k(x)}{u^2}\frac{R_-(x,u)}{1-R_+(x,u)R_-(x,u)e^{-2k_0 Lk(x)u}}[e^{-k_0 k(x)(i-0.5)\Delta u}-e^{-k_0 k(x)(i+0.5)\Delta u}]dx\,du , \\
A_{km} &= I^a_{|k-m|}+I^b_{S+m-k}+I^b_{S+k-m}+I^c_{2S-m-k-1}+I^d_{m+k+1} .
\end{aligned}
\tag{7}
$$

Here, Ei_2 is the second exponential integral as defined by Abramowitz and Stegun [12]. This formulation only requires the evaluation of $7S$ double integrals instead of the $5S^2$ triple integrals that would be necessary if we simply inserted Eq. (5) into Eq. (6), leading to large savings in computer time.

III. RESULTS

Figure 1 shows the lowest-order trapping factor g_0 for a Doppler line shape and $k_0L=5$. g_0 increases most when both walls are highly reflecting, but does not increase much when one reflection coefficient is very high and the other is low. Actually, a slab where one reflection coefficient is 1 and the other is 0 can be replaced by a slab of width $2L$ [13]. A slab where both walls have the reflectivity R roughly has an effective length $L/(1-R)$. This can become very large for large R, so that g_0 can also become much larger than in the case of only one reflecting wall (where the maximum effective length is $2L$).[2]

In a slab with transparent walls and a Doppler line shape, the trapping factors for the higher-order modes are related to the trapping factor for the lowest-order mode roughly by $g_j=1+(g_0-1)m_0/m_j$ (the relation $g_j/g_0=m_0/m_j$ is strictly valid in the limit of infinite g_0), where $m_0=1.025$, $m_1=2.4$, and $m_2=3.9$ [14]. One could now think that this relation would stay the same in a slab with reflecting walls. Figure 2 shows the trapping factors g_0 and g_1 when $R_+=1$ and R_- is varied; we compare the results of this relation to our numerical results. We see that this relation breaks down completely as R_- is increased; as a matter of fact, the higher-order trapping factors are almost independent of the reflection coefficient. This result is somewhat surprising at first glance, but can, for low opacities, be explained by the following physical picture: if we have low opacity and high reflection coefficients, the excited-state distribution tends to become practically uniform within a very short time. This happens because the photons can fly through the vapor for long distances (due to the low opacity), and will be reflected several times before reabsorption. The point of reabsorption is then almost independent of the point of emission, and the points of reabsorption will be distributed uniformly throughout the slab. Even when the initial distribution is sharply peaked at the center of the slab, we will get a constant excited-state distribution (which has roughly the shape of the lowest-order mode) within a time that is determined by the decay time of the higher-order modes for a slab of width k_0L, independent of any wall reflections. Thus, g_j must be practically independent of R. The average number of reabsorptions (which is approximately equal to g_0) is determined by both the vapor opacity and the wall reflection coefficient, so that g_0 strongly depends on wall reflections. Further simulations have shown that, at high opacities also, the dependence of g_j on R is very weak, even when g_j is quite large. For $k_0L=100$, a Doppler line shape, and $R_+=1$, g_1 increases only by 45% (from 90 to 130) when R_- is increased from 0 to 0.98, while g_0 increases by 1500%

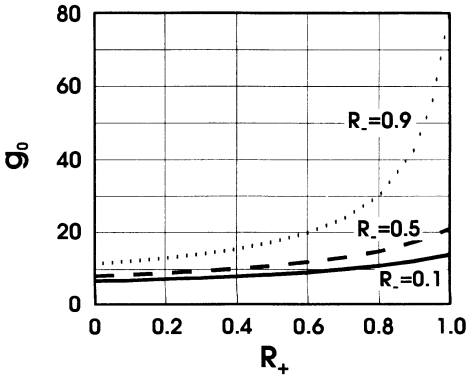

FIG. 1. Lowest-order trapping factor g_0 for specularly reflecting walls as a function of R_+, the reflection coefficient at $L/2$, for a Doppler line shape with $k_0L=5$ for three different values of R_-, the reflection coefficient at $z=-L/2$.

[2]Although a slab with $R_+=1$ and $R_-=0$ can be replaced by an equivalent slab of width $2L$, only the even modes of this equivalent slab can exist. This means that g_j of the cell with the one mirrored wall corresponds to g_{2j} in the equivalent slab.

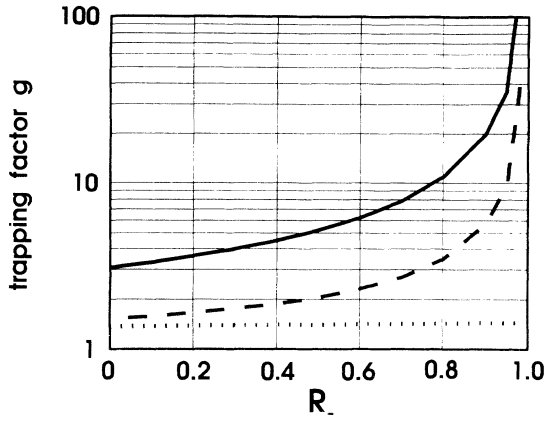

FIG. 2. Trapping factors g_0 and g_1 as a function of R_- for $R_+=1$, and a Doppler line shape with $k_0L=1$: g_0 exact (solid), g_1 exact (dotted), and g_1 by relation $g_1=1+(g_0-1)m_0/m_1$ (dashed). (m_1 here corresponds to m_2 in van Trigt's notation; see the text.)

(from 390 to 6200). It also turned out that, even at high opacities, the shape of the lowest-order mode is practically uniform when both wall reflectivities are high.

We note furthermore that the *area* of the higher-order modes is almost zero in the case that both R_+ and R_- are very large (Fig. 3). This follows directly from the orthogonality of the modes and the fact that the lowest-order mode is almost uniform for large R. Now it can be shown [5] that the number of photons leaving the slab

$$J(t)\propto\sum_j\frac{\alpha_j}{g_j}\exp\left[-\frac{t}{g_j\tau}\right]\int_{-L/2}^{L/2}\Psi_j(z)dz\ . \tag{8}$$

Since the integral (i.e., the area of the mode) is very small for higher-order modes, and the expansion coefficients α_j cannot become much larger than α_0 [only positive $n(z)$ of Eq. (2) are physically meaningful], the influence of these modes on $J(t)$ is usually small. Exceptions are either when many higher-order modes are excited, or when $g_j\ll g_0$ and $\alpha_j\approx\alpha_0$. In those cases, higher-order modes can be important at early times.

If $R_+\neq R_-$, the reflection coefficients can have a larger influence on the higher-order modes. If one wall reflects strongly ($R_+=1$) and the other rather weakly, the higher-order trapping factors have about the same values as for two highly reflecting walls (see Fig. 2). However, g_0 for only one highly reflecting wall is much smaller (since the effective cell length is smaller), so that the relative influence of the higher-order modes is larger. If we have $k_0L=1$, $R_+=1$, and $R_-=0$, we calculate $g_2=1.18$, while for $R_+=R_-=0.995$, we get $g_2=1.19$—even though g_0 in the first case is only 3.02, while it is 149.2 in the latter case. Furthermore, the area of the higher-order modes is now much larger than in the case of two highly reflecting walls (see Fig. 4) so that the higher-order modes can influence $J(t)$ more easily [see Eq. (8)].

Our result (5) permits the inclusion of frequency-dependent reflection coefficients. However, the linewidth of a resonance line usually is only several GHz, and the optical properties of reflecting materials will rarely change within such a small frequency range. If more than one resonant transition is present, the excited-state distributions can be computed by the method of either [10] or [13]; in both cases we combine results for the single lines (either the Green's functions or the trapping factors and eigenmodes) and can assume R to be frequency independent within *each* resonant line.

More important, the reflection coefficient may depend on the angle of incidence. If the reflecting material is a metallic mirror, the reflection coefficient is almost independent of the angle of incidence. This can be used to somewhat simplify the expressions for the A_{km} matrix elements; in that case, $I_i^c/R_+=I_i^d/R_-$, so we have $2S$ integrals less to compute. As will be shown, one can approximate these mirrors by diffusely reflecting walls with tolerable error, but since our formalism allows us to compute specular reflection faster than diffuse reflection, there no longer is any reason for making such an approximation. The number of integrals that have to be evaluated for diffusely reflecting walls is proportional to S^2, while for specularly reflecting walls, it is proportional to S. Especially for multilayer dielectric mirrors and for metallic mirrors coated with dielectric layers, the reflection coefficient can depend significantly on the angle of incidence. Accurate results can be obtained by a full evaluation of Eq. (7).

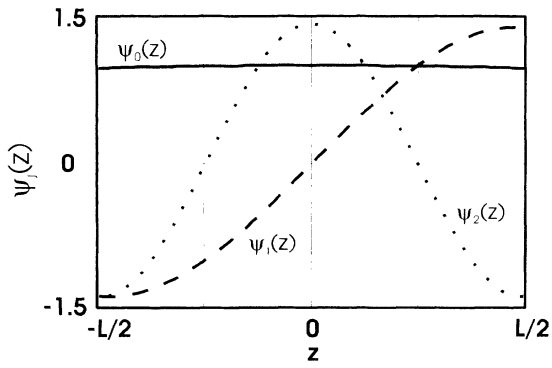

FIG. 3. Eigenmodes $\psi(z)$ for $R_+=R_-=0.99$, and a Doppler line shape with $k_0L=1$.

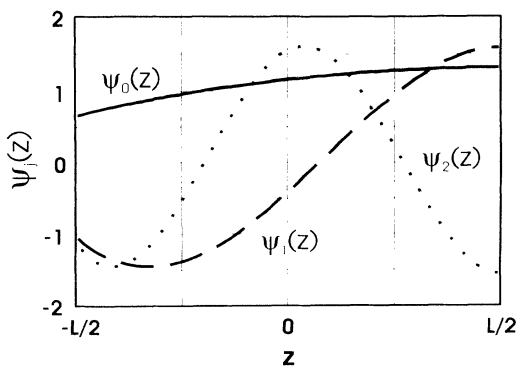

FIG. 4. Eigenmodes $\psi(z)$ for $R_+=1$, $R_-=0$, and a Doppler line shape with $k_0L=1$.

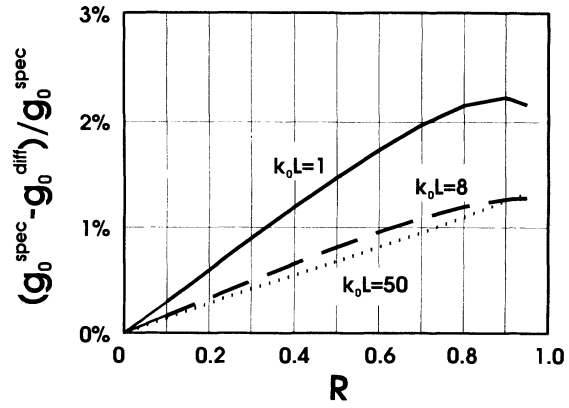

FIG. 5. Relative difference between diffusely and specularly reflecting walls in the lowest-order trapping factor for a Doppler line shape as a function of $R=R_+=R_-$ for three different values of the center-of-line opacity k_0L.

Finally, we can now compare the results for diffusely and specularly reflecting walls. We do not expect the difference between those two cases to be very large. At very high opacities, the many absorption-reemission processes diffuse the radiation, regardless of the kind of reflection at the wall. At very low opacities, the trapping factors cannot change by much anyway [10]. Figure 5 shows the difference in g_0 as a function of R $(=R_+=R_-)$ for low, intermediate, and high opacities for a Doppler line shape. The difference is largest in the region of comparatively low opacities and becomes significantly smaller at very high opacities. The difference is rather small for the shown example; it is below 3%. Further computations show the maximum difference to be 10% for a Doppler line shape and 8% for a Lorentzian line shape for the case of very low opacity combined with high reflectivity ($R>0.9$) so that $g_0\approx 1.5-1.8$ (e.g., $k_0L=0.003$, $R=0.99$ and a Doppler line shape). For $k_0L>0.5$, the error stays below 3% for a Doppler line shape and below 6% for a Lorentzian line shape. These errors are usually tolerable, so that the often-used method of approximating specularly reflecting walls by diffusely reflecting walls [10,15] can now be justified. One could even use specularly reflecting walls in the rare cases when the walls are actually diffuse, since we can now compute specularly reflecting walls faster.

IV. SUMMARY AND CONCLUSION

In summary, we have derived the Green's function for radiation trapping in a slab with specularly reflecting boundaries; the reflection coefficients can be different at the two boundaries and can depend on angle and frequency. We also gave a method for its efficient evaluation. Higher-order modes influence the temporal behavior of the emergent radiation if only one wall of the slab is highly reflecting, but not when both walls are highly reflecting. The difference in the lowest-order trapping factor between diffuse and specular reflection is rather small. Specular reflection can now be computed considerably faster than diffuse reflection. Hence, we suggest using the present approach both for specular reflection (where it is exact) and as an approximation for diffuse reflection.

ACKNOWLEDGMENTS

This work was done for the European Space Agency under ESTEC Contract No. 9516/91/NL/PB(SC). Additional financial support from the Jubiläumsstiftung der Gemeinde Wien is gratefully acknowledged.

[1] A. G. Mitchell and M. W. Zemansky, *Resonance Radiation and Excited Atoms* (Cambridge University Press, Cambridge, England, 1961).
[2] A. Corney, *Atomic and Laser Spectroscopy* (Oxford University Press, Oxford, 1977).
[3] J. A. Gelbwachs, IEEE J. Quantum Electron. **24**, 1266 (1988).
[4] T. Holstein, Phys. Rev. **72**, 1212 (1947).
[5] A. F. Molisch, B. P. Oehry, and G. Magerl, J. Quant. Spectrosc. Radiat. Transfer **48**, 377 (1992).
[6] M. A. Weinstein, J. Appl. Phys. **33**, 587 (1962).
[7] G. B. Tkachuk, Opt. Spectrosc. (USSR) **17**, 139 (1964).
[8] J. H. Ingold, J. Appl. Phys. **39**, 5834 (1968).
[9] J. H. Ingold, J. Appl. Phys. **41**, 94 (1970).
[10] T. M. Colbert and B. L. Wexler, Phys. Rev. A **47**, 2156 (1993).
[11] L. M. Biberman, Zh. Eskp. Teor. Fiz. **17**, 416 (1947).
[12] *Handbook of Mathematical Functions,* edited by M. Abramowitz and I. A. Stegun (Dover, New York, 1965).
[13] A. F. Molisch, B. P. Oehry, W. Schupita, and G. Magerl, Opt. Commun. **90**, 245 (1992).
[14] C. van Trigt, Phys. Rev. **181**, 97 (1969); Phys. Rev. A **13**, 726 (1976).
[15] H. van Tongeren and J. Heuvelmans, J. Appl. Phys. **45**, 3844 (1974).